Asymptotic Structure of Rich Methane-Air Flames

K. SESHADRI*

Center for Energy and Combustion Research, Department of Mechanical and Aerospace Engineering, University of California at San Diego, La Jolla, CA 92093-0411, USA

X. S. BAI

Division of Fluid Mechanics, Department of Heat and Power Engineering, Lund Institute of Technology, S 221 00 Lund, Sweden

and

H. PITSCH

Center for Turbulence Research, Stanford University, Stanford, CA 94305-3030, USA

The asymptotic structure of unstrained, laminar, fuel-rich, premixed methane flame is analyzed by using a reduced chemical-kinetic mechanism made up of three global steps. Analysis is carried out for values of equivalence ratio greater than 1.3. The flame structure is presumed to comprise three zones: an inert preheat zone, a thin reaction zone, and a post-flame zone. In contrast to previous asymptotic analyses of lean flames and moderately rich flames, where the reaction zone of these flames was presumed to be made up of two layers, for rich flames analyzed here all chemical reaction are presumed to take place in one layer. The structure of the reaction zone of rich flames is obtained by integrating two second order ordinary differential equations, one giving the consumption of fuel and the other the consumption of oxygen. For values of equivalence ratio greater than 1.3, burning velocities obtained from the asymptotic analysis are found to agree reasonably well with those obtained using a chemical-kinetic mechanism made up of elementary reactions.

INTRODUCTION

Burning velocities of unstrained premixed methane flames obtained using chemical-kinetic mechanisms made up of elementary reactions show that for lean and near stoichiometric reactant mixtures with equivalence ratio, ϕ, less than 1.1, the burning velocity increases with increasing ϕ [1]. For moderately rich reactant mixtures with ϕ roughly between 1.1 and 1.3, the burning velocity decreases rapidly with increasing ϕ [1]. For rich mixtures with ϕ greater than 1.3, the burning velocity decreases slowly with increasing ϕ [1]. These results were obtained using the so-called C_1-mechanism, C_2-mechanism, and the C_3 mechanism. In the C_1-mechanism/C_2-mechanism/C_3-mechanism, elementary reactions comprising compounds made up of two/three/four or more carbon atoms are excluded. Numerical calculations carried out using chemical-kinetic mechanisms made up of elementary reactions show that the structure of lean flames, moderately rich flames, and rich flames are not the same. For this reason, previous rate-ratio asymptotic analyses of near stoichiometric and lean methane flames [2–6] were different from rate-ratio asymptotic analysis of moderately rich flames [7]. These asymptotic studies successfully predicted the increases in the value of the burning velocity with increasing ϕ for near stoichiometric and lean methane flames, and the rapid decreases in the value of the burning velocity with increasing ϕ for moderately rich flames. The asymptotic analysis for moderately rich flames failed to predict the slow decreases in the value of the burning velocity with increasing ϕ for $\phi > 1.3$. Here, an asymptotic analysis is developed for obtaining the burning velocity of rich methane flames.

Previous asymptotic analyses of near stoichiometric flames, lean flames and moderately rich methane flames were carried out after introducing the approximation that the reaction zone of these flames is made up of two layers; an inner layer and an oxidation layer [2–7]. In the inner layer, methane is completely consumed and CO and H_2 are main compounds formed. In the

* Corresponding author. E-mail: seshadri@mae.ucsd.edu

COMBUSTION AND FLAME 127:2265–2277 (2002)

Published by Elsevier Science Inc.

0010-2180/02/$–see front matter
PII 0010-2180(01)00327-3

oxidation layer of these flames O_2, CO, and H_2 are consumed. In these previous analyses the characteristic temperature of the inner layer was presumed to be given by T^0 [2–7]. The inner layer temperature was obtained from a balance between chain-branching reactions and chain-breaking reactions [6]. Its value is less than the adiabatic temperature, T_b. In the oxidation layer, the temperature increases from T^0 to T_b [2–7]. The analysis of moderately rich flames showed that with increasing values of ϕ, T^0 approaches T_b, and the approximation that the reaction zone is made up of two layers breaks down for even higher equivalence ratio. Hence, in the present asymptotic analysis all chemical reactions are presumed to take place in one layer. The characteristic temperature of this layer is the adiabatic temperature T_b. Appendix A shows structures of a lean flame, a moderately rich flame, and a rich flame. These structures were calculated using the C_2-mechanism. Net rates of production of various species in these flames were obtained. They clearly show that the reaction zone of lean flames and moderately rich flames are made up of two layers, while the reaction zone of rich flames is made up of one layer.

Previous asymptotic analyses of near stoichiometric, lean, and moderately rich methane flames were carried out employing reduced chemical-kinetic mechanisms derived from the C_1-mechanism. For rich flames analyzed here, the elementary reaction $CH_3 + CH_3 = C_2H_6$, that leads to the C_2-chain, is found to be the principal step by which CH_3 is consumed (see Appendix A). Hence, the present asymptotic analysis is carried out employing a reduced mechanism derived from the C_2-mechanism.

REDUCED MECHANISM

The C_2-mechanism employed here is made up of reactions (1)-(61) shown in Table 1.1 of Ref. [8]. The species CH_4, O_2, C_2H_6, C_2H_5, C_2H_4, C_2H_3, C_2H_2, C_2H, H_2O, CO_2, CH_3, CH_2, CH, CH_2O, CHO, CO, H_2, HO_2, H_2O_2, O, OH, and H appear in this C_2-mechanism. A reduced five-step chemical-kinetic mechanism is deduced from the C_2-mechanism after introducing steady-state approximations for C_2H_6, C_2H_5, C_2H_4, C_2H_3, C_2H_2, C_2H, CH_2, CH, CH_2O, CHO, HO_2, H_2O_2, O, and OH. This reduced five-step mechanism is written as

$$CH_4 + H = CH_3 + H_2, \quad \text{(Ia)}$$

$$2\,CH_3 + O_2 = 2CO + 3\,H_2, \quad \text{(Ib)}$$

$$CO + H_2O = CO_2 + H_2, \quad \text{(II)}$$

$$H + H + M = H_2 + M, \quad \text{(III)}$$

$$O_2 + 3H_2 = 2H + 2H_2O. \quad \text{(IV)}$$

Global step Ib is different from that employed in a previous study of moderately rich methane flames [7]. In this previous study the elementary reaction $CH_3 + O = CH_2O + H$ was found to be the main path by which CH_3 is consumed, whereas in the present study the main path by which CH_3 is consumed is found to be $CH_3 + CH_3 = C_2H_6$ (see Appendix A). This is the reason for the difference between the global step Ib employed in the present analysis and that used in the previous analysis of moderately rich methane flames [7]. Global step Ib is deduced by beginning with the reaction, $CH_3 + CH_3 = C_2H_6$ and eliminating the reaction rates of the elementary steps $C_2H_6 + H = C_2H_5 + H_2$, $C_2H_5 = C_2H_4 + H$, $C_2H_4 + H = C_2H_3 + H_2$, $C_2H_3 = C_2H_2 + H$, $C_2H_2 + O = CH_2 + CO$, $CH_2 + O_2 = CO + OH + H$, $OH + H = O + H_2$ from the source terms of the steady state species C_2H_6, C_2H_5, C_2H_4, C_2H_3, C_2H_2, CH_2, and O [9].

Table 1 shows the elementary reactions considered to be the major contributors to the rates of the global steps of the reduced mechanism. Symbols *f* and *b* appearing in the first column of Table 1, respectively, identify the forward and backward steps of a reversible elementary reaction *n*. The backward steps of reactions (34), (35), (36), and (37) are not included in the mechanism shown in Table 1.1 of Ref. [8]. Therefore, they are neglected in the asymptotic analysis. The backward steps of reactions (1), and (5) are neglected in the asymptotic analysis because numerical calculations show that their influence on burning velocities is small for $1.3 < \phi < 2.5$. Rate data for the elementary steps are identical to those shown in Table 1.1 of Ref. [8]. Reaction rate coefficients k_n of the elementary reactions are calculated by using the expression

TABLE 1

Rate data for elementary reactions employed in the asymptotic analysis

Number	Reaction	B_n	α_n	E_n
1f	$O_2 + H \rightarrow OH + O$	2.000E + 14	0.00	70.30
f	$H_2 + O \rightarrow OH + H$	5.060E + 04	2.67	26.3
2b	$H + OH \rightarrow O + H_2$	2.222E + 04	2.67	18.29
3f	$H_2 + OH \rightarrow H_2O + H$	1.000E + 08	1.60	13.80
3b	$H + H_2O \rightarrow OH + H_2$	4.312E + 08	1.60	76.46
4f	$OH + OH \rightarrow H_2O + O$	1.500E + 09	1.14	0.42
4b	$O + H_2O \rightarrow OH + OH$	1.473E + 10	1.14	71.09
5f[a]	$H + O_2 + M \rightarrow HO_2 + M$	2.300E + 18	−0.80	0.00
18f	$CO + OH \rightarrow CO_2 + H$	4.400E + 06	1.50	−3.10
18b	$H + CO_2 \rightarrow OH + CO$	4.956E + 08	1.50	89.76
34f[b]	$CH_3 + H \rightarrow CH_4$ k_0	6.257E + 23	−1.80	0.00
	k_∞	2.108E + 14	0.00	0.00
35f	$CH_3 + O \rightarrow CH_2O + H$	7.000E + 13	0.00	0.00
36f[b]	$CH_3 + CH_3 \rightarrow C_2H_6$ k_0	1.270E + 41	−7.00	11.56
	k_∞	3.613E + 13	0.00	0.00
37f	$CH_3 + O_2 \rightarrow CH_2O + OH$	3.400E + 11	0.00	37.40
38f	$CH_4 + H \rightarrow CH_3 + H_2$	2.200E + 04	3.00	36.60
38b	$CH_3 + H_2 \rightarrow CH_4 + H$	8.391E + 02	3.00	34.56

Units are moles, cubic centimeters, seconds, kJoules, Kelvin.

[a] Third body collision efficiencies are [M] = 6.5[CH_4] + 1.5[CO_2] + 0.75[CO] + 0.4[N_2] + 6.5[H_2O] + 0.4[O_2] + 1.0[Other].

[b] For reaction 34f and reaction 36f: $k = F\, k_\infty k_0[p/(\mathcal{R}T)]/\{k_\infty + k_0[p/(\mathcal{R}T)]\}$, where $\log_{10} F = \log_{10} F_c/\{1 + (\log_{10}(k_0[p/(\mathcal{R}T)]/k_\infty)/\hat{N})^2\}$, $\hat{N} = 0.75 - 1.27 \log_{10} F_c$. For reaction 34f $F_c = 0.577 \exp[-T/2370.0]$. For reaction 36f $F_c = 0.38 \exp[-T/73.0] + 0.62 \exp[-T/1180.0]$.

$k_n = B_n T^{\alpha_n} \exp[-E_n/(\mathcal{R}T)]$, where T denotes the temperature and $\mathcal{R}$ is the universal gas constant. The quantities B_n, α_n, and E_n are the frequency factor, the temperature exponent, and the activation energy of the elementary reaction n. The concentration of the third body C_M is calculated by using the relation $C_M = [pW/(\mathcal{R}T)] \sum_{i=1}^{n} \eta_i Y_i/W_i$ where p denotes the pressure, W the molecular weight of the mixture and Y_i, W_i, and η_i are respectively, the mass fraction, the molecular weight, and the chaperon efficiency of species i. Chaperon efficiencies are shown in Table 1. The rates of reactions (4) and (18) are not used in the analysis.

Reaction rates of the global steps w_k in the five-step mechanism (k = Ia-IV), are

$$\begin{aligned} w_{\mathrm{Ia}} &= -w_{34\mathrm{f}} + w_{38\mathrm{f}} - w_{38\mathrm{b}}, \\ w_{\mathrm{Ib}} &= 0.5\, w_{35\mathrm{f}} + w_{36\mathrm{f}} + 0.5\, w_{37\mathrm{f}}, \\ w_{\mathrm{II}} &= w_{18\mathrm{f}} - w_{18\mathrm{b}}, \\ w_{\mathrm{III}} &= w_{5\mathrm{f}} + w_{34\mathrm{f}}, \\ w_{\mathrm{IV}} &= w_{1\mathrm{f}} - 0.5\, w_{35\mathrm{f}} + 0.5\, w_{37\mathrm{f}}. \end{aligned} \tag{1}$$

Here w_n is the reaction rate of elementary reaction n. A number of elementary reactions in addition to those shown in Eq. 1 contribute to the rates of the global steps of the reduced mechanism. Contributions of these additional reactions are neglected because they are found to be small.

Steady-state concentration of O is required for calculating the global rates of the reduced mechanism. To make the analysis simple the elementary reactions (2) and (3) are presumed to maintain partial equilibrium. A previous study has shown that burning velocities, calculated after introducing these partial equilibrium approximations, are reasonably accurate [1]. The partial equilibrium approximations give

$$C_{\mathrm{O}} = \frac{C_{\mathrm{H_2O}} C_{\mathrm{H}}^2}{K_2 K_3 C_{\mathrm{H_2}}^2}, \tag{2}$$

where C_i is the molar concentration of species i, and K_n is the equilibrium constant of the elementary step n.

Steady-state approximations are introduced for H and CH_3. This gives the three-step mechanism

$$CH_4 + O_2 \rightleftharpoons CO + H_2 + H_2O, \qquad (Ia'')$$

$$CO + H_2O \rightleftharpoons CO_2 + H_2, \qquad (II'')$$

$$O_2 + 2H_2 \rightleftharpoons 2H_2O. \qquad (III'')$$

Reaction rates of the global steps w_k in the three-step mechanism (k = Ia″–III″), are

$$\begin{aligned} w_{Ia''} &= w_{Ia} = -w_{34f} + w_{38f} - w_{38b}, \\ w_{II''} &= w_{II} = w_{18f} - w_{18b}, \\ w_{III''} &= w_{III} = w_{5f} + w_{34f}. \end{aligned} \qquad (3)$$

Steady-state concentrations of H and CH_3 are calculated using the algebraic equations

$$\begin{aligned} -2w_{1f} + 2w_{5f} + w_{34f} + w_{35f} - w_{37f} \\ + w_{38f} - w_{38b} = 0, \end{aligned} \qquad (4)$$

$$w_{34f} + w_{35f} + 2w_{36f} + w_{37} - w_{38f} + w_{38b} = 0.$$

The three-step mechanism, k = Ia″, II″, III″, is employed in the asymptotic analysis.

FORMULATION

Steady propagation of a planar, laminar flame under adiabatic conditions is considered. The Mach number is presumed to be small. Mass conservation gives $\rho v = \rho_u s_L$, where ρ is the density, v the gas velocity, and s_L the burning velocity. Subscript u refers to the initial conditions in the unburnt reactant mixture. Lewis numbers, $Le_i = \lambda/(\rho c_p D_i)$, for species i are assumed to be constants. Here λ is the thermal conductivity, c_p the mean specific heat at constant pressure, and D_i the diffusion coefficient of species i. The heat capacity is presumed to be constant. Diffusion velocities of species are presumed to be given by Fick's Law [10]. The non-dimensional species balance equations and the energy conservation equation are

$$\begin{aligned} \frac{dX_i}{dx} - \frac{1}{Le_i}\frac{d^2X_i}{dx^2} &= \sum_{k=Ia}^{III} (\nu_{i,k}\omega_k), \\ \frac{d\tau}{dx^2} - \frac{d^2\tau}{dx^2} &= \sum_{k=Ia}^{III} (Q_k\omega_k), \end{aligned} \qquad (5)$$

where $x \equiv \int_0^{x'} (\rho v c_p/\lambda)dx'$ and x' is the spatial coordinate. The origin $x = 0$ is taken to coincide with the location of the inner reactive-diffusive zone. The quantity $\nu_{i,k}$ is the stoichiometric coefficient of species i in the global step k of the reduced mechanism. The value of $\nu_{i,k}$ is positive if species i appears on the right side of global step k and negative if it appears on the left side. The dependent variables X_i and τ are defined as

$$X_i \equiv \frac{Y_i W_F}{Y_{F,u} W_i}, \quad \tau \equiv \frac{T - T_u}{T_c - T_u}. \qquad (6)$$

X_i is the normalized mass fraction of species i, τ is the normalized temperature, and subscript F refers to the fuel. $Y_{F,u}$ is the initial value of Y_F in the unburnt reactant mixture, T_c is the temperature of burnt gases obtained by introducing the approximation that the chemical reaction takes place by the one-step overall process $CH_4 + 2O_2 = CO_2 + 2H_2O$. From Eq. 6 it follows that $C_i = (\rho Y_{F,u}/W_F)X_i$. The non-dimensional reaction rates w_k and heats of reaction Q_k are defined as

$$\omega_k \equiv \frac{\lambda W_F w_k}{c_p Y_{F,u} \rho_u^2 {s_L}^2}, \quad Q_k \equiv \frac{Y_{F,u}(-\Delta H_k)}{c_p (T_c - T_u) W_F}, \qquad (7)$$

where $(-\Delta H_k)$ is the heat release in the global step k. From the definition of Q_k it follows that $Q_{Ia''} + Q_{II''} + Q_{III''} = 1$. Their values are $Q_{Ia''} = 0.3458$, $Q_{II''} = 0.0514$, and $Q_{III''} = 0.6028$.

The asymptotic structure of the premixed flame is presumed to comprise a preheat zone of thickness of the order of unity, a thin reaction zone of thickness of the order of $\epsilon \ll 1$, and a post-flame zone. The preheat zone is located upstream of the reaction zone. It is presumed to be inert. All chemical reactions take place in the reaction zone. The post-flame zone is located downstream of the reaction zone. In this zone chemical reactions are in equilibrium and the temperature is equal to its adiabatic value T_b. The equilibrium products in the post-flame zone are presumed to comprise CO_2, H_2O, O_2, CO, H_2, and N_2. The equivalence ratio, ϕ, for methane flames is given by $\phi = 4Y_{F,u}/Y_{O_2,u}$, where $Y_{O_2,u}$ is the initial value of Y_{O_2} in the unburnt reactant mixture. For p = 1 bar, T_u = 300K, and $1.0 < \phi < 2.5$; values of T_c T_b, and

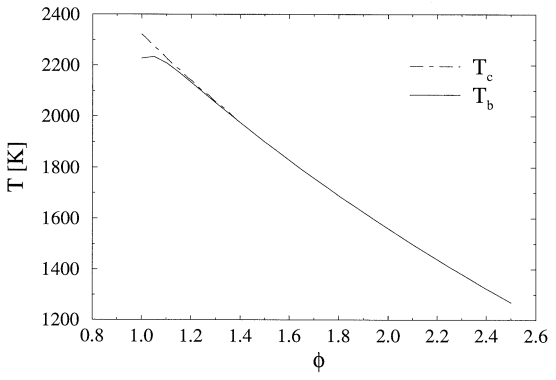

Fig. 1. The temperature for complete combustion, T_c, and equilibrium temperature in the post-flame zone, T_b, as functions of the equivalence ratio, ϕ, for $p = 1$ bar and $T_u = 300$ K.

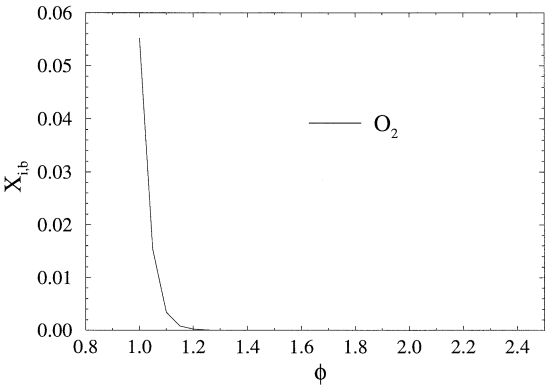

Fig. 3. The normalized mass fraction of oxygen, $X_{O_2,b}$ in the post-flame zone as a function of the equivalence ratio, ϕ, for $p = 1$ bar and $T_u = 300$ K.

mass fractions of equilibrium products $Y_{i,b}$ are obtained. Figures 1, 2, and 3 show temperatures and normalized mass fractions of various species in the post-flame zone. Figure 1 shows T_c and T_b, Fig. 2 shows values of $X_{i,b}$, $i = CO_2$, H_2O, CO, and H_2, and Fig. 3 shows $X_{O_2,b}$. In the analysis $X_{CO_2,b}$, $X_{H_2O,b}$, $X_{CO,b}$, and $X_{H_2,b}$, are presumed to be of the order of unity, and $X_{O_2,b}$ is presumed to be small.

In the preheat zone, X_F and X_{O_2} are of the order of unity. They are obtained by neglecting the reaction terms in the balance equations. Thus

$$X_F = 1 - \exp(Le_F x),$$
$$X_{O_2} = X_{O_2,u}\,[1 - \exp(Le_{O_2} x)], \tag{8}$$

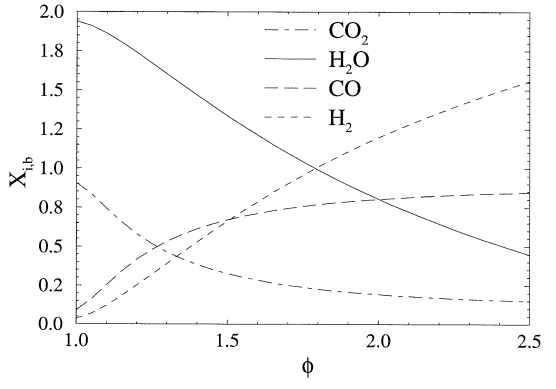

Fig. 2. The normalized mass fractions $X_{CO_2,b}$, $X_{H_2O,b}$, $X_{CO,b}$, $X_{H_2,b}$ in the post-flame zone as functions of the equivalence ratio, ϕ, for $p = 1$ bar and $T_u = 300$ K.

where the origin of the coordinate system is so chosen that $x = 0$ at the reaction zone. $X_{O_2,u}$ is the initial value of X_{O_2} in the unburnt reactant mixture.

ASYMPTOTIC ANALYSIS OF THE REACTION ZONE

In the asymptotic analysis of the reaction zone, the convective terms in the species balance equations and in the energy conservation equation shown in Eq. 5 are neglected because they are presumed to be small in comparison to the diffusive terms and the reactive terms. Balance equation for X_{O_2}, X_F, and X_{CO} are

$$\frac{1}{Le_{O_2}}\frac{d^2X_{O_2}}{dx^2} = \omega_{5f} + \omega_{38f} - \omega_{38b},$$
$$\frac{1}{Le_F}\frac{d^2X_F}{dx^2} = -\omega_{34f} + \omega_{38f} - \omega_{38b}, \tag{9}$$
$$\frac{1}{Le_{CO}}\frac{d^2X_{CO}}{dx^2} = \omega_{18f} - \omega_{18b} + \omega_{34f} - \omega_{38f} + \omega_{38b},$$

where use is made of Eq. 3. The values of X_{CO_2}, X_{H_2O}, and X_{H_2} can be obtained from the following conservation equations for the elements carbon, oxygen and hydrogen.

$$\frac{d^2}{dx^2}\left(\frac{X_F}{Le_F}+\frac{X_{CO}}{Le_{CO}}+\frac{X_{CO_2}}{Le_{CO_2}}\right)=0,$$

$$\frac{d^2}{dx^2}\left(2\frac{X_{O_2}}{Le_{O_2}}+2\frac{X_{CO_2}}{Le_{CO_2}}+\frac{X_{CO}}{Le_{CO}}+\frac{X_{H_2O}}{Le_{H_2O}}\right)=0,$$

$$\frac{d^2}{dx^2}\left(2\frac{X_F}{Le_F}+\frac{X_{H_2O}}{Le_{H_2O}}+\frac{X_{H_2}}{Le_{H_2}}\right)=0. \tag{10}$$

Energy conservation gives

$$\frac{d^2}{dx^2}\left[\tau+Q_{III''}\frac{X_{O_2}}{Le_{O_2}}+(1-2Q_{III''})\frac{X_F}{Le_F}+Q_{II''}\frac{X_{CO}}{Le_{CO}}\right]=0. \tag{11}$$

Using numerical values for Q_k the result

$$\frac{d^2}{dx^2}\left[\tau+0.6028\frac{X_{O_2}}{Le_{O_2}}-0.2056\frac{X_F}{Le_F}+0.0514\frac{X_{CO}}{Le_{CO}}\right]=0, \tag{12}$$

is obtained.

The expansions

$$X_{O_2}=\epsilon Le_{O_2}y_{O_2}+O(\epsilon^2),$$

$$X_F=\epsilon Le_F y_F+O(\epsilon^2),$$

$$X_i=X_{i,b}+\epsilon Le_i y_i+O(\epsilon^2),$$

$$i=H_2O,\ CO_2,\ CO,\ H_2, \tag{13}$$

$$X_H=R_H Le_H y_H+O(R_H{}^2),$$

$$X_{CH_3}=R_{CH_3}Le_{CH_3}y_{CH_3}+O(R_{CH_3}{}^2),$$

$$\tau=\tau_b-\epsilon t+O(\epsilon^2),$$

are introduced. Here $\tau_b=(T_b-T_u)/(T_c-T_u)$. The dependent variables y_i, $i=O_2$, F, H_2O, CO_2, CO, H_2, H, CH_3, and t are presumed to be of the order of unity. The expansion parameters $\epsilon \ll 1$, $R_H \ll 1$, and $R_{CH_3} \ll 1$ are presumed to be given by

$$\epsilon=\frac{k_{34f,b}X_{H_2,b}}{k_{36f,b}K_{38,b}Le_F},$$

$$R_H=\frac{k_{1f,b}{}^2X_{H_2,b}Le_{O_2}{}^2}{k_{34f,b}k_{38f,b}K_{38,b}Le_F{}^2Le_H}, \tag{14}$$

$$R_{CH_3}=\frac{k_{1f,b}{}^2X_{H_2,b}Le_{O_2}{}^2}{k_{36f,b}k_{38f,b}K_{38,b}Le_F{}^2Le_{CH_3}}$$

Here rate constants, $k_{n,b}$ and equilibrium constants $K_{n,b}$ are evaluated at the adiabatic temperature, T_b. The analysis is carried out in the distinguished limit of $\sigma \gg 1$, and $\omega \gg 1$, where

$$\sigma=\epsilon/R_{CH_3};\quad \omega=\epsilon/R_H. \tag{15}$$

The quantity σ is a measure of the ratio of the normalized mass fractions of O_2 and CH_3 in the reaction zone, and ω is a measure of the ratio of the normalized mass fractions of O_2 and H in the reaction zone.

Analysis of the reaction zone is carried out using an independent variable ζ given by

$$x=\epsilon\zeta. \tag{16}$$

Use of Eqs. 13, 14, and 16 in Eq. 9 gives the differential equations

$$\frac{d^2y_{O_2}}{d\zeta^2}=L\,(g_{5f}\kappa y_{O_2}y_H+y_F y_H-y_{CH_3}),$$

$$\frac{d^2y_F}{d\zeta^2}=L\,(-\mu^2 y_H y_{CH_3}+y_F y_H-y_{CH_3}). \tag{17}$$

The differential equation for CO is not required for obtaining the burning velocity. The eigenvalue L is presumed to be of the order of unity. It is given by

$$L=\frac{Y_{F,u}}{s_L{}^2W_F}\left(\frac{\lambda_b}{c_{p,b}}\right)\left(\frac{\rho_b}{\rho_u}\right)^2 k_{38f,b}\epsilon^2R_H Le_F Le_H. \tag{18}$$

The parameters κ and μ are presumed to be of the order of unity. They are given by

$$\kappa=\frac{k_{5f,b}C_{M,b}Le_{O_2}}{k_{38f,b}Le_F};\quad \mu=\frac{k_{1f,b}Le_{O_2}}{k_{38f,b}Le_F}. \tag{19}$$

The density ρ and thermal conductivity λ are evaluated at $T=T_b$. Changes in their values with changes in temperature in the reaction zone are neglected. Changes in values of rate constants of all elementary reactions, except those of reactions 1f and 5f, with temperature are also neglected. The quantities

$$g_{1f} = \frac{k_{1f}}{k_{1f,b}} = \exp\left[-8455.62\left(\frac{1}{T} - \frac{1}{T_b}\right)\right],$$

$$g_{5f} = \frac{k_{5f}C_M}{k_{5f,b}C_{M,b}} = \exp\left[1.80T_{ref}\left(\frac{1}{T} - \frac{1}{T_b}\right)\right], \quad (20)$$

give changes in values of k_{1f} and $k_{5f}C_M$ with temperature. Here the approximation $T^{\alpha_n} = (T_{ref})^{\alpha_n}\exp(\alpha_n)\exp(-\alpha_n T_{ref}/T)$ is applied to the rate data shown in Table 1, where T_{ref} is a reference temperature. For simplicity, values of Y_i appearing in the definition of $C_{M,b}$ are presumed to be equal to $Y_{i,b}$. Errors introduced from use of this approximation are presumed to be small. Asymptotic analysis that includes changes in values of ρ, λ, and rate constants of all elementary reactions with temperature is described in the Appendix B.

Boundary conditions for Eq. 17 are obtained by matching the profiles of oxygen and fuel in the reaction zone with those in the post-flame zone. In the limit $\zeta \to \infty$, Eq. (17) is required to satisfy the boundary conditions

$$\frac{dy_{O_2}}{d\zeta} = 0, \quad \frac{dy_F}{d\zeta} = 0, \quad (21)$$

and $y_{O_2} = 0$ and $y_F = y_{F,\infty}$. If backward steps of all elementary reactions are included in the analysis, the fuel will be completely consumed in the post-flame zone and the mass fractions of equilibrium products are shown in Figs. 2 and 3. For large negative values of ζ, the profiles of y_{O_2} and y_F must match with those in the preheat zone given by Eq. 8. In the limit $\zeta \to -\infty$, the boundary conditions

$$\frac{dy_{O_2}}{d\zeta} = -X_{O_2,u}; \quad \frac{dy_F}{d\zeta} = -1, \quad (22)$$

are obtained. Equation 17 is invariant to translation of the coordinate system. To fix the origin, boundary conditions are applied at some arbitrary value ζ_0, where $-\zeta_0$ is large. Boundary conditions at ζ_0 are $y_{O_2} = -X_{O_2,u}\zeta_0$ and $y_F = -\zeta_0$ in addition to those given by Eq. 22. Fuel is found to leak from the reaction zone into the post-flame zone, while leakage of oxygen is found to be negligible. The fuel leakage, $y_{F,\infty}$ is given by the asymptotic value of y_F in the limit $\zeta \to \infty$. The values of the eigenvalue L and $y_{F,\infty}$ are so chosen that the boundary condition Eq. 21 is satisfied.

Equations that give the steady-state concentrations of H and CH_3 are obtained by use of Eqs. 13 and 14 in Eq. 4. The steady-state concentrations are

$$\begin{aligned} &-2g_{1f}\mu y_{O_2}y_H + 2g_{5f}\kappa y_{O_2}y_H + \mu^2 y_H y_{CH_3} \\ &+ \psi y_H^2 y_{CH_3} - \chi y_{O_2}y_{CH_3} \\ &+ y_F y_H - y_{CH_3} = 0 \\ &\mu^2 y_H y_{CH_3} + \psi y_H^2 y_{CH_3} + 2\mu^2 y_{CH_3}^2 \\ &+ \chi y_{O_2}y_{CH_3} - y_F y_H + y_{CH_3} = 0 \end{aligned} \quad (23)$$

The parameters χ and ψ in Eq. 23 are presumed to be of the order of unity. They are given by

$$\chi = \frac{k_{34f,b}k_{37f,b}Le_{O_2}}{k_{36f,b}k_{38f,b}Le_F};$$

$$\psi = \frac{k_{1f,b}{}^4 k_{35f,b}X_{H_2O,b}Le_{O_2}{}^4}{k_{34,b}{}^2 k_{38f,b}{}^3 K_{2,b}K_{3,b}K_{38,b}X_{H_2,b}Le_F{}^4} \quad (24)$$

To obtain the temperature in the reaction zone, the expansions given by Eq. 13 are introduced into Eq. 12 and integrated twice. The constants of integration are evaluated by imposing the constraints that at $\zeta \to \infty$, derivatives with respect to ζ of t, y_{O_2}, and y_F vanish, values of t and y_{O_2} vanish, and the value of y_F is $y_{F,\infty}$. This gives $t - t_\infty = 0.6028\, y_{O2} - 0.2056\,(y_F - y_{F,\infty})$, where the approximation $Q_{II} \ll 1$ is used, and t_∞ is the value of t in the limit $\zeta \to \infty$. The ad hoc approximation $t_\infty = 0$ is introduced in the analysis. The expansion for τ in Eq. 13 gives $T = T_b - \epsilon t(T_c - T_u)$. By using this expansion for T, the value of $1/T - 1/T_b$ in Eq. 20 is evaluated from the equation

$$\frac{1}{T} - \frac{1}{T_b} = \frac{\epsilon[0.6028y_{O_2} - 0.2056\,(y_F - y_{F,\infty})]\,(T_c - T_u)}{T_b{}^2}. \quad (25)$$

Equation 25 is used to evaluate g_{1f} and g_{5f} in Eq. 20. Equation 17 is integrated numerically and

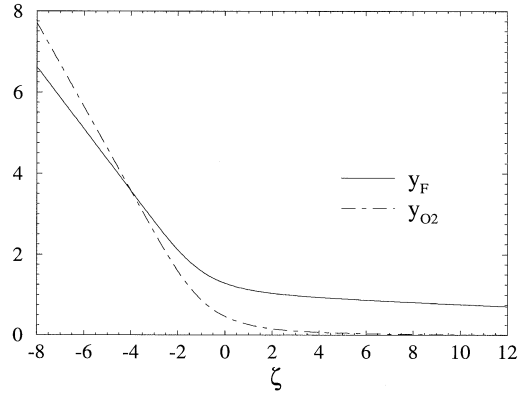

Fig. 4. Profiles of y_F and y_{O_2} for $p = 1$ bar, $T_u = 300$ K and $\phi = 2.0$.

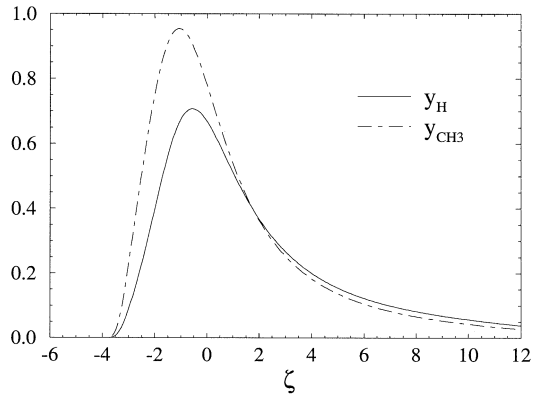

Fig. 5. Profiles of y_H and y_{CH_3} for $p = 1$ bar, $T_u = 300$ K and $\phi = 2.0$.

the burning velocity is obtained. Results are given in the following section.

RESULTS

Equations derived in the previous sections are used to obtain flame structures and burning velocities at $p = 1$ bar and $T_u = 300$ K. Values of Le_i are $Le_F = Le_{CH_3} = 0.97$, $Le_{O_2} = 1.1$, and $Le_H = 0.2$. The value of $(\lambda_b/c_{p,b})$ in Eq. 18 is obtained from $(\lambda_b/c_{p,b}) = 2.58 \times 10^{-5}$ $(T_b/298)^{0.7}$ kg/(m.s) [11]. The molecular weight of the mixture W is taken to be a constant and it is evaluated in the post-flame zone; and $T_{ref} = 1{,}900$ K.

Figure 4 shows profiles of y_F and y_{O_2} obtained from integration of Eq. 17 for $\phi = 2.0$. The asymptotic values of y_F and y_{O_2}, for large values of ζ, give the amount fuel and oxygen leaking from the reaction zone into the post-flame zone. Figure 4 shows that fuel leaks from the reaction zone into the post-flame zone while leakage of oxygen is negligible. Figure 5 shows profiles of the steady-state species y_H and y_{CH_3} obtained from Eq. 23 for $\phi = 2.0$. Figure 6 shows the eigenvalue L, and fuel-leakage $y_{F,\infty}$ for various values of ϕ. The fuel-leakage is small. It increases with increasing ϕ. The burning velocity is obtained from L using Eq. 18.

Figure 7 shows that burning velocities obtained from asymptotic analysis that includes changes in values of k_{1f} and $k_{5f}C_M$ with changes in temperature agree well with those obtained from asymptotic analysis, described in Appendix B, where changes in values of ρ, λ and all rate constants with temperature are included. To test the accuracy of s_L obtained from the asymptotic analysis, numerical calculations were performed by using the three-step mechanism, $k =$ Ia″, II″, III″, employing only the rate data shown in Table 1. The burning velocities calculated by using the asymptotic analysis agree very well with those calculated by using the three-step mechanism. To test the accuracy of s_L obtained from the asymptotic analysis, and from the three-step mechanism numerical calculations were performed using the C_2 mechanism. Burning velocities were obtained. They are shown in Fig. 7 for $1 < \phi < 2.5$. For ϕ greater than 1.7, s_L obtained from asymptotic analysis agrees well with that obtained using the C_2 mechanism. For ϕ less than 1.7, the difference between the value of s_L calculated from asymptotic analysis and

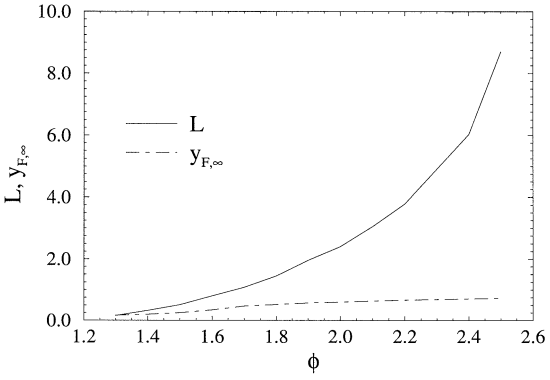

Fig. 6. The eigenvalue L, and fuel-leakage $y_{F,\infty}$ versus the equivalence ratio, ϕ, for $p = 1$ bar and $T_u = 300$.

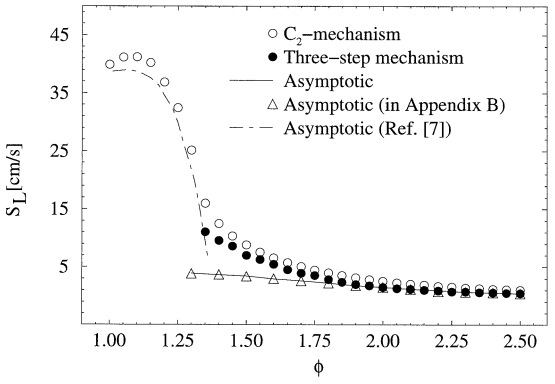

Fig. 7. Burning velocities, s_L (cm/s) versus the equivalence ratio, ϕ. The solid line represents burning velocities obtained from asymptotic analysis that includes changes in values of k_{1f} and $k_{5f}C_M$ with changes in temperature, the triangles represent burning velocities obtained from asymptotic analysis that includes changes in values of ρ, λ, and all rate constants with temperature. The open circles represent burning velocities obtained from numerical calculations carried out using the C_2 mechanism. The filled circles represent burning velocities obtained from numerical calculations carried out using the reduced three-step mechanism. The chain line represents burning velocities obtained from previous asymptotic analysis of moderately rich flames [7].

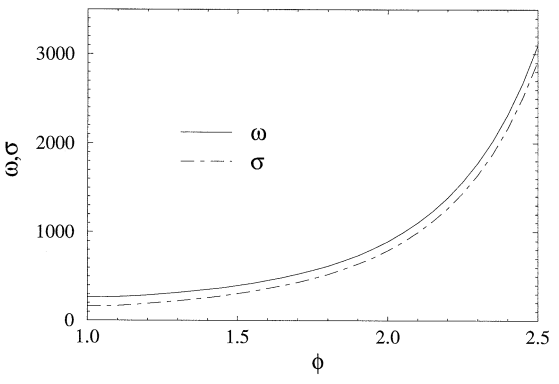

Fig. 9. The parameters, σ, and ω versus ϕ for $p = 1$ bar and $T_u = 300$K.

that obtained from the C_2 mechanism increases as ϕ decreases. These differences are attributed to the various approximations introduced in the analysis including the neglect of changes in the values of CO and H_2 in the reaction zone. Figure 7 shows that s_L obtained from previous asymptotic analysis of moderately rich flames [7] agrees well with that calculated by using the C_2 mechanism for $1 < \phi < 1.3$, but cannot predict the transition to rich flames.

Figures 8, 9, and 10 show ϵ, σ, ω, κ, μ, χ, and ψ for various values of ϕ. Figure 8 shows that the characteristic thickness of the reaction zone, represented by ϵ, increases with increasing ϕ. Figure 9 shows that σ and ω are large for all values of ϕ. Therefore, steady-state approximations for CH_3 and H are expected to be accurate. Figure 10 shows the parameters κ, μ, χ, and ψ. The value of ψ is very small. This indicates that the influence of elementary reaction 35f on the structure and burning velocity of rich flames is small. This reaction, however, is found to have a significant influence on the concentration of radicals in stoichiometric flames and lean flames.

CONCLUDING REMARKS

The present asymptotic analysis together with previous asymptotic analyses of near stoichiometric and lean flames [2–4, 6] and moderately

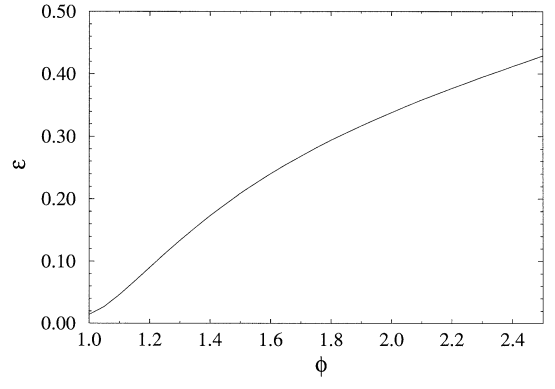

Fig. 8. Expansion parameter ϵ versus ϕ for $p = 1$ bar and $T_u = 300$ K.

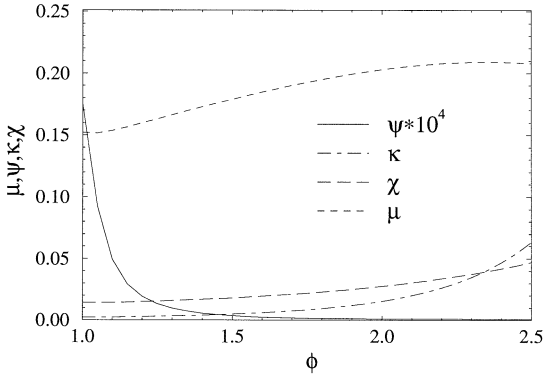

Fig. 10. The parameters, κ, μ, χ, and ψ versus ϕ for $p = 1$ bar and $T_u = 300$ K.

rich flames [7], give a complete description of the structure of methane flames for all values of ϕ. For near stoichiometric and lean flames the structure of the oxidation layer was obtained by analyzing the consumption of CO and H_2 [2–4, 6]. For moderately rich flames the structure of the oxidation layer was obtained by analyzing the consumption of O_2 [7]. In these previous analyses, leakage of methane from the reaction zone into the post-flame zone was found to be negligible. For lean flames and stoichiometric flames and moderately rich flames, the values of the characteristic temperature at the inner layer, T^0, is less than the adiabatic temperature, T_b. For rich flames CH_4 and O_2 are consumed in a single layer. The characteristic temperature of this layer is T_b. In rich flames, the fuel leaks from the reaction zone into the post-flame zone. These are the main differences between the analysis of the asymptotic structure of rich flames and analyses of the asymptotic structures of lean flames and moderately rich flames.

The authors thank Professor Norbert Peters for helpful discussions. The authors thank Dr. Reinhard Seiser for preparing Figs. 14 through 19. The research was supported by the National Science Foundation through Grant # CTS-9900631. Dr. X. S Bai was supported by the Swedish Research Council for Engineering Sciences (TFR). Dr. H. Pitsch was supported by the DFG.

APPENDIX A

To test the accuracy of the approximations employed in the asymptotic analysis, the structure of a lean flame with $\phi = 0.8$, the structure of a moderately rich flame with $\phi = 1.2$, and the structure of a rich flame with $\phi = 1.9$ are calculated using the C_2-mechanism. Figures 11, 12, and 13 show profiles of mass fractions of CH_4, O_2, CO_2, CO, and H_2 and the temperature profile for $\phi = 0.8$, $\phi = 1.2$, and $\phi = 1.9$, respectively. Figure 11 shows that in a lean flame, CH_4 is completely consumed in the reaction zone, the mass fractions of CO and H_2 first increase and then decrease. In this flame O_2 is consumed but its mass fraction in the reaction zone is much larger than that of CO. The profiles of CH_4, CO, and H_2 in the moderately

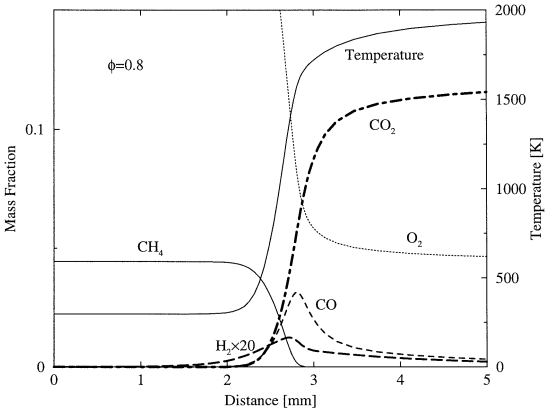

Fig. 11. Profiles of mass fractions of CH_4, O_2, CO_2, CO, and H_2, and the temperature profile in a lean flame with $\phi = 0.8$, $p = 1$ bar, and $T_u = 300$ K.

rich flame shown in Fig. 12 are similar to those in the lean flame. In the moderately rich flame O_2 is consumed and its mass fraction in the reaction zone in comparable to that of CO. Figure 13 shows that in a rich flame O_2 is completely consumed in the reaction zone, while CH_4 leaks from the reaction zone into the post-flame zone. The mass fraction of H_2 increases. The decrease in the value of the mass fraction of CO in the post-flame zone, from its maximum value in the reaction zone, is very small. Thus, the structures of lean flames, moderately rich flames, and rich flames are not the same. Numerical calculations were carried out using the C_2-mechanism including the backward steps of all elementary reactions. The profiles of all species in the lean flame and in the moder-

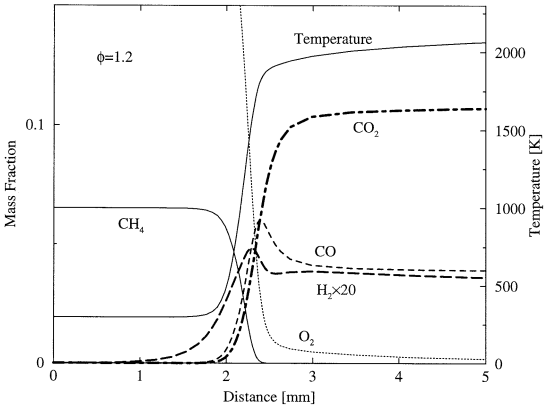

Fig. 12. Profiles of mass fractions of CH_4, O_2, CO_2, CO, and H_2, and the temperature profile in a moderately rich flame with $\phi = 1.2$, $p = 1$ bar and $T_u = 300$ K.

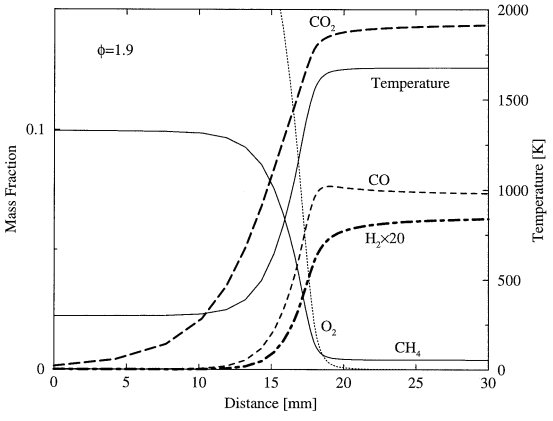

Fig. 13. Profiles of mass fractions of CH_4, O_2, CO_2, CO, and H_2, and the temperature profile in a rich flame with $\phi = 1.9$, $p = 1$ bar, and $T_u = 300$ K.

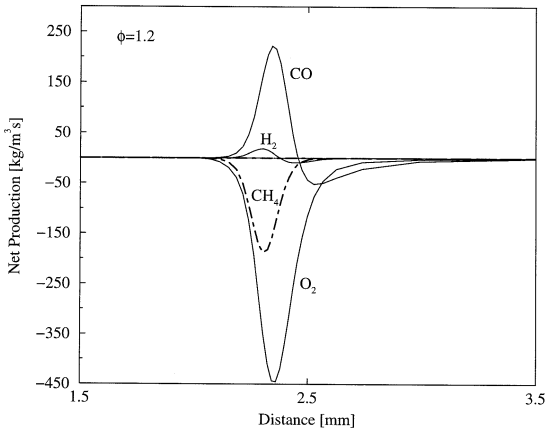

Fig. 15. Net rates of production of CH_4, O_2, H_2, and CO in a moderately rich flame with $\phi = 1.2$, $p = 1$ bar, and $T_u = 300$ K.

ately rich flame were similar to those shown in Figs. 11, and 12. The profiles of all species in the rich flame, except that of the fuel, were similar to those shown in Fig. 13. The profile of the fuel in the preheat zone and the reaction zone obtained including backward steps of all elementary reactions was similar to that shown in Fig. 13. In the post-flame zone the profile of fuel calculated including backward steps of all elementary reactions was found to decrease slowly with increasing distance from the reaction zone. Thus there is slow consumption of fuel in the post-flame zone eventually leading to equilibrium products.

Figures 14, 15, and 16 show net rates of production of CH_4, O_2, H_2, and CO in a lean flame, a moderately rich flame and a rich flame respectively. In these figures a species is produced if its net rate of production is positive and it is consumed if its net rate of production is negative. Figures 14, 15, and 16 show that CH_4 and O_2 are consumed everywhere. Figures 14 and 15 show that in the lean flame and in the moderately rich flame, CO is formed in the region where CH_4 is consumed. Consumption of CO follows consumption of CH_4. This justifies approximations employed in previous asymptotic analyses that the reaction zones of lean flames and moderately rich methane flames are made up of two layers [2–7]. Figure 16 shows that CO is produced everywhere. Consumption of CH_4 and O_2 and production of

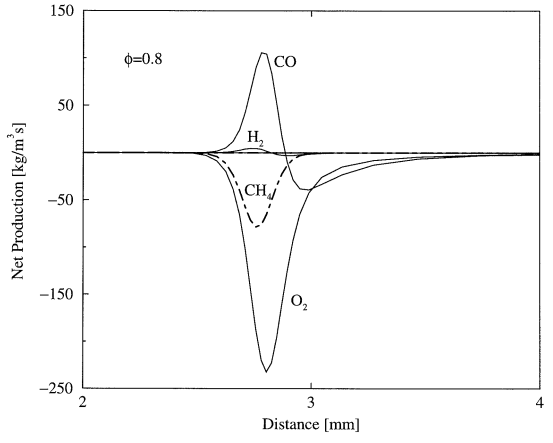

Fig. 14. Net rates of production of CH_4, O_2, H_2, and CO in a lean flame with $\phi = 0.8$, $p = 1$ bar, and $T_u = 300$ K.

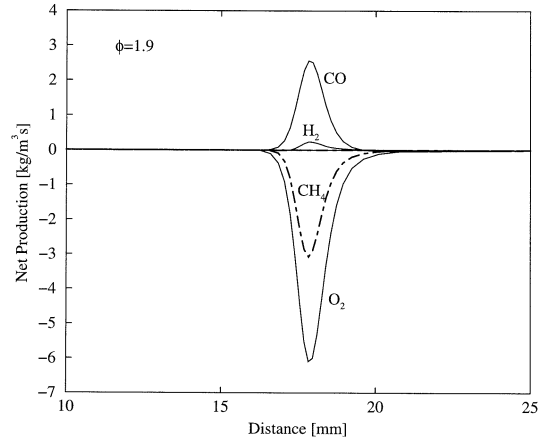

Fig. 16. Net rates of production of CH_4, O_2, H_2, and CO in a rich flame with $\phi = 1.9$, $p = 1$ bar, and $T_u = 300$ K.

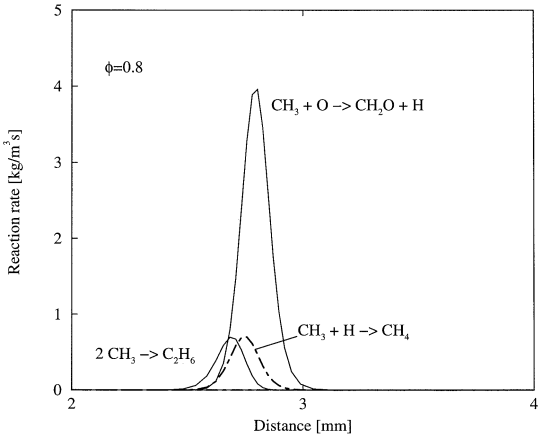

Fig. 17. Rate of consumption of CH_3 by various elementary reactions in a lean flame with $\phi = 0.8, p = 1$ bar, and $T_u = 300$ K.

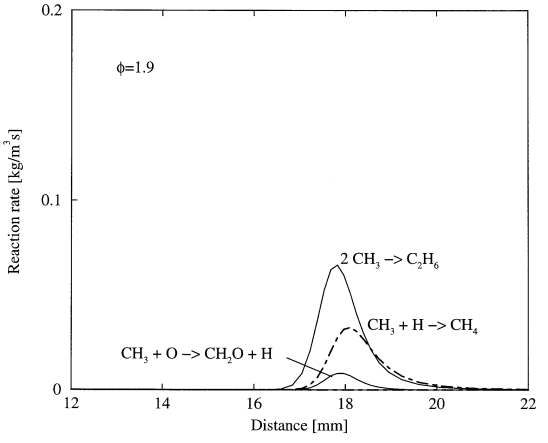

Fig. 19. Rate of consumption of CH_3 by various elementary reactions in a rich flame with $\phi = 1.9, p = 1$ bar, and $T_u = 300$ K.

CO and H_2 take place in the same region. Hence, in the present asymptotic analysis of rich flames all chemical reactions are presumed to take place in one layer.

Figures 17, 18, and 19 show reaction rates of the elementary steps $CH_3 + O = CH_2O + H$, $CH_3 + H = CH_4$, and $CH_3 + CH_3 = C_2H_6$. They give rates of consumption of CH_3 by these reactions. Figures 17 and 18 show that in the lean flame and in the moderately rich flame the rate of consumption of CH_3 by the elementary reaction 35f is the highest. This justifies approximations introduced in previous asymptotic analyses of lean flames and moderately rich flames that, to the leading order, the rate of consumption of CH_3 is given by the rate of reaction 35f [2–7]. Figures 17 and 18 show that the rates of consumption of CH_3, by the elementary reactions 34f and 36f, in moderately rich flames are higher than those in lean flames. Hence, in previous asymptotic analyses of near stoichiometric and lean flames the contribution of reaction 34f was included as a perturbation [2–6]. In previous asymptotic analyses of moderately rich flames the contribution of reaction 34f to the rate of consumption of CH_3 was presumed to be of the same order as that of reaction 35f [7].

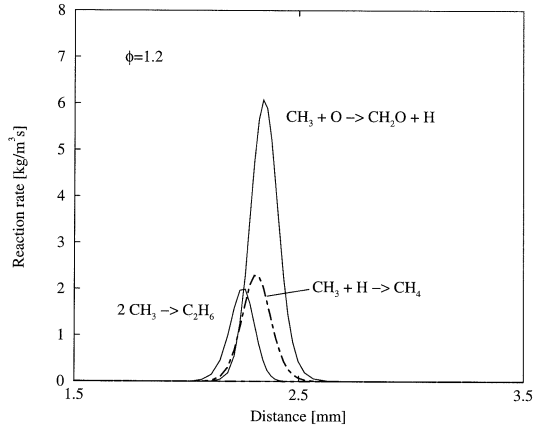

Fig. 18. Rate of consumption of CH_3 by various elementary reactions in a moderately rich flame with $\phi = 1.2, p = 1$ bar and $T_u = 300$ K.

Figure 19 shows that in the rich flame the rate of consumption of CH_3 by the elementary reaction 36f is the highest. The rate of consumption of CH_3 by the elementary reaction 35f is very small in comparison to that by reaction 36f. Thus, in the present asymptotic analysis reaction 36f is presumed to be the principal step by which CH_3 is consumed.

APPENDIX B

The influence of changes in values of ρ, λ, and rate constants of all elementary reactions with temperature on the burning velocity is investigated. These changes are given by

$$G_L = \frac{(\lambda/c_p)\rho^2}{(\lambda_b/c_{p,b})\rho b^2}$$

$$= \exp\left[(2-\alpha_T)\,T_{ref}\left(\frac{1}{T}-\frac{1}{T_b}\right)\right],$$

$$g_{34f} = \frac{k_{34f}}{k_{34f,b}} = \exp\left[734.0\left(\frac{1}{T}-\frac{1}{T_b}\right)\right],$$

$$g_{35f} = \frac{k_{35f}K_{2,b}K_{3,b}}{k_{35f,b}K_2K_3}$$

$$= \exp\left[-6573.25\left(\frac{1}{T}-\frac{1}{T_b}\right)\right],$$

$$g_{36f} = \frac{k_{36f}}{k_{36f,b}} = \exp\left[1035.0\left(\frac{1}{T}-\frac{1}{T_b}\right)\right],$$

$$g_{37f} = \frac{k_{37f}}{k_{37f,b}} = \exp\left[-4498.44\left(\frac{1}{T}-\frac{1}{T_b}\right)\right],$$

$$g_{38f} = \frac{k_{38f}}{k_{38f,b}}$$

$$= \exp\left[-(4402.21+3T_{ref})\left(\frac{1}{T}-\frac{1}{T_b}\right)\right],$$

$$g_{38b} = \frac{k_{38b}}{k_{38b,b}}$$

$$= \exp\left[-(4156.84+3T_{ref})\left(\frac{1}{T}-\frac{1}{T_b}\right)\right]. \quad (26)$$

The quantity $\alpha_T = 0.7$ accounts for changes in λ/c_p with temperature. The quantities g_{34f} and g_{36f} are obtained from plots of $\ln k_{34f}$ versus $1/T$ and $\ln k_{36f}$ versus $1/T$ for $700 < T < 2000$ and $p = 1$ bar.

The differential equations for y_{O_2} and y_F are written as

$$\frac{d^2y_{O_2}}{d\zeta^2} = LG_L\,(g_{5f}\kappa y_{O_2}y_H + g_{38f}y_Fy_H - g_{38b}y_{CH_3}),$$

$$\frac{d^2y_F}{d\zeta^2} = LG_L\,(-g_{34f}\mu^2y_Hy_{CH_3} + g_{38f}y_Fy_H - g_{38b}y_{CH_3}). \quad (27)$$

Equations that give the steady-state concentrations of y_H and y_{CH_3} are

$$-2g_{1f}\mu y_{O_2}y_H + 2g_{5f}\kappa y_{O_2}y_H + g_{34f}\mu^2y_Hy_{CH_3} + g_{35f}\psi y_H{}^2y_{CH_3} - g_{37f}\chi y_{O_2}y_{CH_3} + g_{38f}y_Fy_H - g_{38b}y_{CH_3} = 0$$

$$g_{34f}\mu^2y_Hy_{CH_3} + g_{35f}\psi y_H{}^2y_{CH_3} + 2g_{36f}\mu^2y_{CH_3}{}^2 + g_{37f}\chi y_{O_2}y_{CH_3} - g_{38f}y_Fy_H + g_{38b}y_{CH_3} = 0. \quad (28)$$

Boundary conditions for Eq. 27 are given by Eqs. 21 and 22. Burning velocities are shown in Fig. 7.

REFERENCES

1. Mauß F., and Peters N., *Reduced Kinetic Mechanisms for Applications in Combustion Systems*, in N. Peters and B. Rogg, Eds. Volume m15 of *Lecture Notes in Physics*, Chapter 5, pp. 58–75. Springer-Verlg, Berlin Heidelberg, 1993.
2. Peters N., and Williams F. A., *Combust. Flame* 68(2): 185–207 (1987)
3. Seshadri K., and Peters N., *Combust. Flame* 81:96–118 (1990)
4. Seshadri K., and Göttgens J., *Reduced Kinetic Mechanisms and Asymptotic Approximations for Methane-Air Flames*, (in M. D. Smooke, Ed.) Volume 384 of *Lecture Notes in Physics*, Chapter 6, pp. 111–136. Springer-Verlag, Berlin Heidelberg, 1991.
5. Bui-Pham M., Seshadri K., and Williams F. A., *Combust. Flame* 89:343–362 (1992)
6. Seshadri K., *Proc. Combust. Institute*, 26:831–846 (1996)
7. Seshadri K., Bai X. S., Pitsch H., and Peters N., *Combust. Flame* 113:589–602 (1998)
8. Peters N., *Reduced Kinetic Mechanisms for Applications in Combustion Systems*, (in Peters N. and Rogg B., Eds.) Volume m15 of *Lecture Notes in Physics*, Chapter 1, pp. 1–13. Springer-Verlag, Heidelberg, 1993.
9. Peters N., *Reduced Kinetic Mechanisms and Asymptotic Approximations for Methane-Air Flames*, in (M. D. Smooke, Ed.) Volume 384 of *Lecture Notes in Physics*, Chapter 3, pp. 48–67. Springer-Verlag, Berlin Heidelberg, 1991.
10. Williams F. A., *Combustion Theory*. Addison-Wesley Publishing Company, Redwood City, CA, 2nd ed. 1985.
11. Smooke M. D., and Giovangigli V., *Reduced Kinetic Mechanisms and Asymptotic Approximations for Methane-Air Flames*, in M. D. Smooke, Ed. Volume 384 of *Lecture Notes in Physics*, Chapter 2, pp. 29–47. Springer Verlag Berlin Heidelberg, 1991.

Received 28 February 2001; revised 22 August 2001; accepted 10 September 2001